

# Short Range Operator Contributions to $0\nu\beta\beta$ decay from LQCD

Henry Monge-Camacho<sup>1,2</sup>

<sup>1</sup> College of William & and Mary

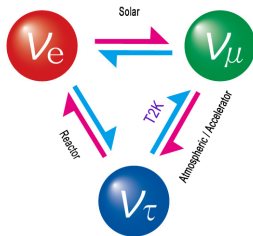
<sup>2</sup>LBNL

36th International Symposium on Lattice Field Theory  
July 24, 2018



U.S. DEPARTMENT OF  
**ENERGY**

# Motivation



Neutrino oscillation between three generations

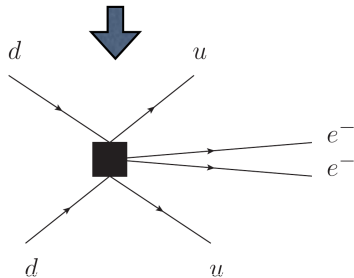


# Motivation

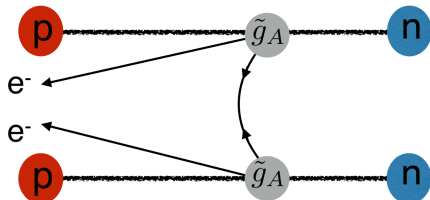
$0\nu\beta\beta$  Half life

$$\frac{1}{T_{1/2}} = G(Q_{\beta\beta}, Z)|M|^2 \eta_{\beta\beta}$$

Experiments focused on  $0^+ \rightarrow 0^+$



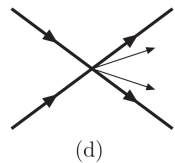
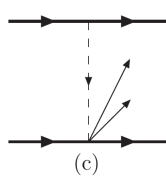
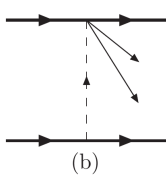
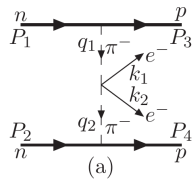
$$\frac{\eta_{\beta\beta}}{\frac{1}{m_e} \sum U_{el} m_l} \quad \text{Light neutrino} \quad \frac{m_N \sum U_{eh} / m_h}{\text{Heavy neutrino}}$$



B. C. Tiburzi, M. L. Wagman, F. Winter, E. Chang, Z. Davoudi, W. Detmold, K. Orginos, M. J. Savage, and P. E. Shanahan (2017). In: *Phys. Rev. D96.5*, p. 054505. arXiv: 1702.02929 [hep-lat]

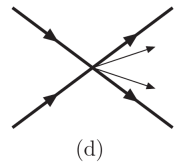
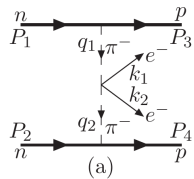
# Contributing Diagrams

G. Prezeau, M. Ramsey-Musolf, and P. Vogel (2003). In: *Phys. Rev.* D68, p. 034016. arXiv: hep-ph/0303205 [hep-ph] used Effective Field Theory to Integrate out heavy modes and obtain the contributing operators are found to be:



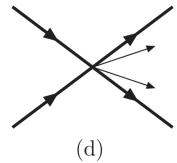
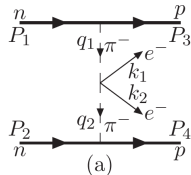
# Contributing Diagrams

G. Prezeau, M. Ramsey-Musolf, and P. Vogel (2003). In: *Phys. Rev.* D68, p. 034016. arXiv: hep-ph/0303205 [hep-ph] used Effective Field Theory to Integrate out heavy modes and obtain the contributing operators are found to be:



# Contributing Diagrams

G. Prezeau, M. Ramsey-Musolf, and P. Vogel (2003). In: *Phys. Rev.* D68, p. 034016. arXiv: hep-ph/0303205 [hep-ph] used Effective Field Theory to Integrate out heavy modes and obtain the contributing operators are found to be:



## Decay Operators

$$\mathcal{O}_{1+}^{++} = (\bar{q}_L \tau^+ \gamma^\mu q_L)(\bar{q}_R \tau^+ \gamma^\mu q_R)$$

$$\mathcal{O}_{2\pm}^{++} = (\bar{q}_R \tau^+ q_L)(\bar{q}_R \tau^+ q_L) + (\bar{q}_L \tau^+ q_R)(\bar{q}_L \tau^+ q_R)$$

$$\mathcal{O}_{3\pm}^{++} = (\bar{q}_L \tau^+ q_L)(\bar{q}_L \tau^+ q_L) + (\bar{q}_R \tau^+ q_R)(\bar{q}_R \tau^+ q_R)$$

$$\mathcal{O}_{4\pm}^{++} = (\bar{q}_L \tau^+ \gamma^\mu q_L \mp \bar{q}_R \tau^+ \gamma^\mu q_R)(\bar{q}_L \tau^+ q_R - \bar{q}_R \tau^+ q_L)$$

$$\mathcal{O}_{5\pm}^{++} = (\bar{q}_L \tau^+ \gamma^\mu q_L \pm \bar{q}_R \tau^+ \gamma^\mu q_R)(\bar{q}_L \tau^+ q_R + \bar{q}_R \tau^+ q_L)$$

# $\pi^- \rightarrow \pi^+$ Matrix Element

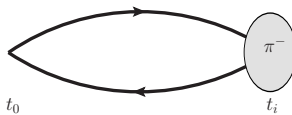
The operators contributing to  $\pi^- \rightarrow \pi^+$  process are  $\mathcal{O}_{1+}^{++}$ ,  $\mathcal{O}_{2+}^{++}$   $\mathcal{O}_{3+}^{++}$  and  $\mathcal{O}'_{1+}^{++}$ ,  $\mathcal{O}'_{2+}^{++}$  (color mixed).

The corresponding 3-point correlation functions are computed as follows:

# $\pi^- \rightarrow \pi^+$ Matrix Element

The operators contributing to  $\pi^- \rightarrow \pi^+$  process are  $\mathcal{O}_{1+}^{++}$ ,  $\mathcal{O}_{2+}^{++}$   $\mathcal{O}_{3+}^{++}$  and  $\mathcal{O}'_{1+}^{++}$ ,  $\mathcal{O}'_{2+}^{++}$  (color mixed).

The corresponding 3-point correlation functions are computed as follows:

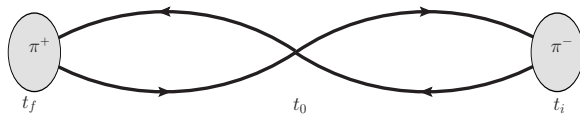


$$\bar{d}\gamma^5 u \rangle$$

# $\pi^- \rightarrow \pi^+$ Matrix Element

The operators contributing to  $\pi^- \rightarrow \pi^+$  process are  $\mathcal{O}_{1+}^{++}$ ,  $\mathcal{O}_{2+}^{++}$   $\mathcal{O}_{3+}^{++}$  and  $\mathcal{O}'_{1+}^{++}$ ,  $\mathcal{O}'_{2+}^{++}$  (color mixed).

The corresponding 3-point correlation functions are computed as follows:

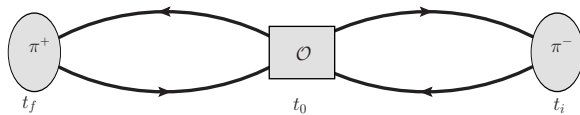


$$\langle \bar{d}\gamma^5 u \quad \bar{d}\gamma^5 u \rangle$$

# $\pi^- \rightarrow \pi^+$ Matrix Element

The operators contributing to  $\pi^- \rightarrow \pi^+$  process are  $\mathcal{O}_{1+}^{++}$ ,  $\mathcal{O}_{2+}^{++}$   $\mathcal{O}_{3+}^{++}$  and  $\mathcal{O}'_{1+}^{++}$ ,  $\mathcal{O}'_{2+}^{++}$  (color mixed).

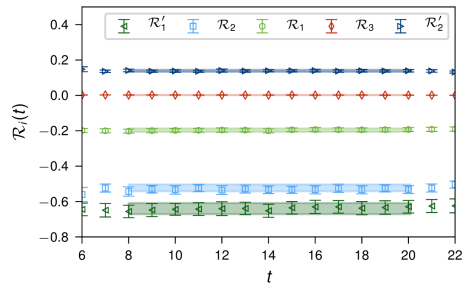
The corresponding 3-point correlation functions are computed as follows:



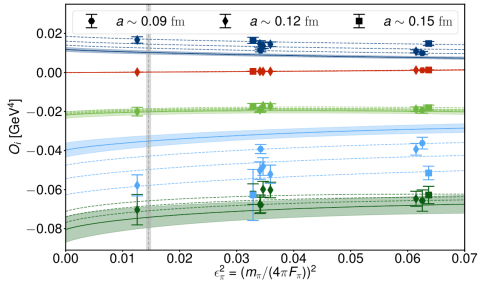
$$\langle \bar{d} \gamma^5 u \quad | \bar{u} \Gamma^1 \textcolor{red}{d} \textcolor{blue}{\bar{u}} \Gamma^2 d | \quad \bar{d} \gamma^5 u \rangle$$

$$\pi^- \rightarrow \pi^+$$

A. Nicholson et al. (2018). In: arXiv: 1805.02634 [nucl-th]



$$\mathcal{R}_i(t) = \frac{a^4 \langle \pi | \mathcal{O}_{i+}^{++} | \pi \rangle}{(a^2 Z_0^\pi)^3} + \mathcal{R}_{e.s.}(t)$$



$$O_1 = \frac{\beta_1 \Lambda_\chi^4}{(4\pi)^2} \left[ 1 + \frac{7}{3} \epsilon_\pi^2 \ln(\epsilon_\pi^2) + c_1 \epsilon_\pi^2 \right]$$

$$O_2 = \frac{\beta_2 \Lambda_\chi^4}{(4\pi)^2} \left[ 1 + \frac{7}{3} \epsilon_\pi^2 \ln(\epsilon_\pi^2) + c_2 \epsilon_\pi^2 \right]$$

$$O_3 = \frac{\beta_3 \Lambda_\chi^4}{\epsilon_\pi^2 (4\pi)^2} \left[ 1 + \frac{4}{3} \epsilon_\pi^2 \ln(\epsilon_\pi^2) + c_3 \epsilon_\pi^2 \right]$$

# $\pi^- \rightarrow \pi^+$ Results

These matrix elements become inputs for nucleon potentials.  
For example:

$$V_i^{nn \rightarrow pp}(|\mathbf{q}|) = -O_i \frac{g_A^2}{4F_\pi^2} \tau_1^+ \tau_2^+ \frac{\sigma_1 \cdot \mathbf{q} \sigma_2 \cdot \mathbf{q}}{(|\mathbf{q}|^2 + m_\pi^2)^2}$$

# Non-perturbative Renormalization

A. Nicholson et al. (2018). In: arXiv: 1805.02634 [nucl-th]

C. C. Chang et al. (2018). In: *Nature* 558.7708, pp. 91–94. arXiv: 1805.12130 [hep-lat]

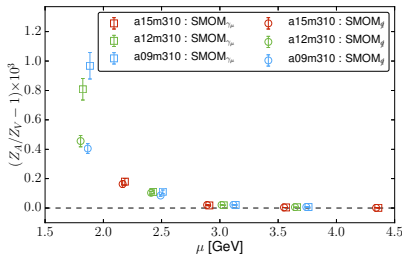


TABLE II. Resulting matrix elements extrapolated to the physical point, renormalized in RI/SMOM and  $\overline{MS}$ , both at  $\mu = 3$  GeV.

$O_i[GeV]^4$	RI/SMOM		$\overline{MS}$
	$\mu = 3$ GeV	$\mu = 3$ GeV	$\mu = 3$ GeV
$O_1$	$-1.96(14) \times 10^{-2}$		$-1.94(14) \times 10^{-2}$
$O'_1$	$-7.21(53) \times 10^{-2}$		$-7.81(57) \times 10^{-2}$
$O_2$	$-3.60(30) \times 10^{-2}$		$-3.69(31) \times 10^{-2}$
$O'_2$	$1.05(09) \times 10^{-2}$		$1.12(10) \times 10^{-2}$
$O_3$	$1.89(09) \times 10^{-4}$		$1.90(09) \times 10^{-4}$

## Method RI-SMOM:<sup>1</sup>

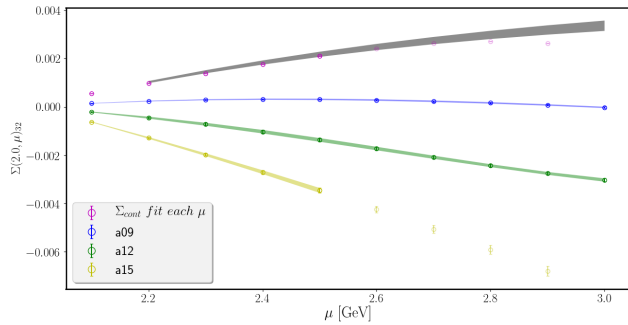
Three Lattice spacings: 0.09, 0.12, 0.15 fm

Projectors:  $\gamma$  and  $q$  show agreement after  $\overline{MS}$  conversion

Step scaling functions are used to handle reduced renormalization windows (0.15)

<sup>1</sup>C. Sturm, Y. Aoki, N. H. Christ, T. Izubuchi, C. T. C. Sachrajda, and A. Soni (2009). In: *Phys. Rev.* D80, p. 014501. arXiv: 0901.2599 [hep-ph]

# Renormalization Constants Running



Renormalization Group  $\Rightarrow$  cont. running  $\Sigma(\mu_1, \mu_2) = Z(\mu_1)Z(\mu_2)^{-1}$

In the Lattice:  $\Sigma(\mu_1, \mu_2, a) = \Sigma(\mu_1, \mu_2)_{cont} + \Delta a^2$

Fit assuming smooth  $\mu$  dependence to obtain  $\Sigma(\mu_1, \mu_2)_{cont}$

R. Arthur and P. A. Boyle (2011). In: *Phys. Rev.* D83, p. 114511. arXiv: 1006.0422 [hep-lat]

# Four-quark Feynman-Hellman Method: $\pi^- \rightarrow \pi^+$

Analog of method implemented for baryons and bilinear currents <sup>2</sup>

$$\partial_\lambda E_\lambda = \langle n | H_\lambda | n \rangle \quad S_\lambda = \lambda \int d^4x \bar{\psi} \Gamma^1 \psi \bar{\psi} \Gamma^2 \psi$$

$$\partial_\lambda E_\lambda$$

For a meson effective mass:

$$\frac{\partial m_{\text{eff}}}{\partial \lambda} \Big|_{\lambda=0} = -\frac{\partial_\lambda C(t+\tau) + \partial_\lambda C(t-\tau) - 2\cosh(m_{\text{eff}}\tau)\partial_\lambda C(t)}{2\tau C(t)\sinh(m_{\text{eff}}\tau)}$$

For long enough t

$$\frac{\partial m_{\text{eff}}}{\partial \lambda} \Big|_{\lambda=0} \approx \frac{\mathcal{J}_{00}}{2E_0^2}$$

$$\partial_\lambda C(t)$$

Matrix element is pulled down with  $\partial_\lambda$

$$N(t) = \int d^4x \left\langle \Omega | T\mathcal{O}(t) \mathcal{J}(x) \mathcal{O}^\dagger(0) | \Omega \right\rangle$$

<sup>2</sup>C. Bouchard, C. C. Chang, T. Kurth, K. Orginos, and A. Walker-Loud (2017). In: *Phys. Rev.* D96.1, p. 014504. arXiv: 1612.06963 [hep-lat]

# Lattice Implementation:

Brute force calculation on small Lattice:

$$\int d^4x \left\langle \Omega | T\mathcal{O}(t) \mathcal{J}(x) \mathcal{O}^\dagger(0) | \Omega \right\rangle = \sum_{y_0 \in V} \left( \pi_t^+ \right)$$

The diagram shows a closed loop consisting of two curved arcs meeting at two circular vertices. The left vertex is shaded gray and contains the text  $\pi_t^+$ . The right vertex is solid black and contains the text  $\pi_0^-$ . Arrows on the arcs indicate a clockwise direction around the loop.

Hubbard-Stratanovich Transformation:

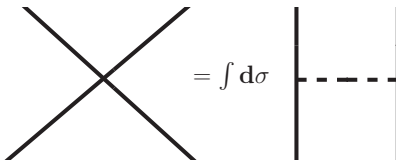
$$e^{-\lambda^2 \int d^4x (\bar{\Psi} \Gamma \Psi)^2} = \alpha \int_{-\infty}^{\infty} d\sigma e^{-\int d^4x \left\{ \frac{\sigma^2}{4} + \lambda i \sigma (\bar{\Psi} \Gamma \Psi) \right\}}$$

D. J. Gross and A. Neveu (1974). In: *Phys. Rev.* D10, p. 3235

R. L. Stratonovich (1957). In: *Doklady Akad. Nauk S.S.R.* 115, p. 1097, J. Hubbard (1959). In: *Phys. Rev. Lett.* 3, pp. 77–80

# Lattice Implementation:

Four-quark is recovered after  $\sigma$  integration:



Numerical implementation:

$$\int d^4x \langle \Omega | T\mathcal{O}(t)\mathcal{J}(x)\mathcal{O}^\dagger(0)|\Omega \rangle = \langle \pi_t^+ | \sum_\sigma \Gamma^1 | \pi_0^- \rangle + \langle \pi_t^+ | \sum_\sigma \Gamma^2 | \pi_0^- \rangle$$

A Feynman diagram illustrating the numerical implementation of a four-quark vertex. It shows a four-quark vertex (a square with internal lines) connected to a loop diagram. The loop consists of two vertices, each with a self-energy insertion. The left vertex is associated with a quark line labeled  $\pi_t^+$  and the right vertex is associated with an antiquark line labeled  $\pi_0^-$ . The loop is closed by two gluon lines, one above and one below the vertices, with arrows indicating the direction of flow.

## Conclusions and Future Work:

Reproduce  $\pi^- \rightarrow \pi^+$  calculation with the new method

Implement calculation using the Hubbard-Stratanovich transformation

Apply method to  $nn \rightarrow pp$  calculation



LBNL: Chia Cheng Chang, André Walker-Loud,

W&M and LLNL: David Brantley

BNL: Enrico Rinaldi

FZJ: Evan Berkowitz

JLab: Bálint Jóo

Liverpool Univ.: Nicolas Garron



LLNL: Pavlos Vranas, Arjun Gambhir

NERSC: Thorsten Kurth

UNC: Amy Nicholson



nVidia: Kate Clark

Funded by: Nuclear Theory for Double-Beta Decay  
and Fundamental Symmetries (DBD Collaboration, D

